SUPPLEMENTARY INFORMATION

Eliminating malaria transmission requires targeting immature and mature gametocytes through lipoidal uptake of antimalarials

Mariska Naude[1,2], Ashleigh van Heerden[1,2], Janette Reader[1,2], Mariëtte van der Watt[2], Jandeli Niemand[1,2], Dorè Joubert[1], Giulia Siciliano[3], Pietro Alano[3], Mathew Njoroge[4], Kelly Chibale[4,5], Esperanza Herreros[6], Didier Leroy[6], Lyn-Marié Birkholtz[1,2,7]*

SUPPLEMENTARY INFORMATION:

1) Supplementary methods
2) Supplementary figures S1 – 7
3) Supplementary files provided:
    1) Supplementary Data S1: Complete dataset of compounds with activity against ABS parasites and gametocytes for meta-analysis.
    2) Supplementary Data S2: Determined activity of 80 MMV compounds screened against ABS parasites, immature and mature gametocytes.
    3) Supplementary Data S3: *In vitro vs* human dose concentrations of compounds
    4) Supplementary Data S4: Target expression profiles of compounds.
    5) Supplementary Data S5: Physicochemical properties of compounds & comparison of various multiclass models performances.
    6) Supplementary Data S6: Exact *p*-values for Figures 3 and 6
    7) Supplementary Figure S1: Differences in activities indicated as fold change between ABS parasites and gametocytes.
    8) Supplementary Figure S2: Parallel evaluation of a select set of compounds against ABS parasites and gametocytes.
    9) Supplementary Figure S3: Morphological evaluation of transgenic parasites.
    10) Supplementary Figure S4: Influence of antimalarial compounds on gametocyte development.
    11) Supplementary Figure S5: Transcript and protein expression of targets of compounds.
    12) Supplementary Figure S6: Machine learning models to validate stage-specific activity profiles of compounds.
    13) Supplementary Figure S7: The contribution of compound uptake through different uptake mechanisms.

SUPPLEMENTARY METHODS

Constitutively expressed luciferase transgenic line

Parasite morphology of the transgenic NF54^{nap} line was assessed by visualizing the ABS parasites across the 48 h cycle and compared to that of NF54^{attB} (wild-type control). The lines' ability to undergo gametocytogenesis was also determined and compared to that of NF54^{attB}. The five gametocyte stages were evaluated for NF54^{nap} over the 10-12 day development period and the viability of these gametocytes confirmed by the formation of male exflagellating centres and the activation of female gametes as before[1,2].

Luciferase enzyme kinetics was analyzed for a mixed population of ABS parasites (6 % parasitemia, 1 % hematocrit) by monitoring the bioluminescent signal over a 1 h timeframe (reading every 10 min). To determine the correlation between the luciferase activity and ABS parasitemia, mixed populations of ABS parasite cultures were prepared at 1-3 % parasitemia (1 % hematocrit). The hematocrit was also evaluated at 1 and 2 % using a 2 % parasitemia.

From the transgenic line the inhibitory concentrations of compounds (IC_{50}) was determined on tightly synchronized ABS parasites (95.17 ± 2.80 % ring stage), >80 % stage II/III immature gametocytes (12.87 ± 1.59 % stage I, 41.6 ± 4.3 % stage II and 37.7 ± 3.9 % stage III gametocytes with ABS parasites effectively removed with both *N*-acetylglucosamine and sorbitol treatment) and >80 % stage V gametocytes (10.0 ± 0.9 % stage IV and 80.30 ± 2.45 % stage V). Luciferase activity on ABS parasites, immature and late-stage gametocytes (in the presence or absence of compounds) was determined by adding 1 mM D-luciferin substrate (0.1 M citric acid and 0.1 M trisodium citrate 2-hydrate, pH 5.5) at a 1:1 ratio at room temperature[3] and detection of resultant bioluminescence at an integration constant of 10 s. Assay quality was also evaluated for signal-to-background (S/B) and signal-to-noise (S/N) ratio, Z'-factor and inter-assay reproducibility via % coefficient of variation (% CV)[4,5].

Effect of therapeutic concentrations of compounds on late-stage gametocytes

For investigating the effect of using therapeutic concentrations of compounds on gametocytes, late-stage gametocytes (>90 % stage IV/V) were produced from *P. falciparum* NF54-*pfs16*-GFP-Luc[6]. Drug treatments were performed on a 'normal'

gametocyte suspension (final concentration of 1 x 10^5 gametocytes/well) and 10 % of the normal gametocyte suspension (final concentration of 1 x 10^4 gametocytes/well) for 48 h under hypoxic conditions at 37 °C. Methylene blue (5 µM) was used as positive control for inhibition. Luciferase activity was measured in 20 µL parasite lysates by adding 50 µL luciferin substrate (Promega Luciferase Assay System) at room temperature and detection of resultant bioluminescence at an integration constant of 10 s.

Inhibition activities against ABS parasites were also determined using SYBR Green I fluorescence. Here, ring-stage NF54 *P. falciparum* (1 % parasitemia, 1 % hematocrit) was treated with compounds at therapeutic concentrations for 48 h at 37 °C[7,8] with chloroquine disulphate (0.5 µM) as positive drug control and dimethyl sulfoxide (DMSO) as negative control. Fluorescence was measured as described above.

Evaluating uptake mechanisms

Inhibition activity (IC_{50}) of only Auphen was determined (before being used in subsequent blocking experiments) against ABS parasites (IC_{50} = 1405 nM) using SYBR Green I fluorescence and gametocytocidal activity on immature gametocytes (> 80 % stage II/III, IC_{50} = 2911 nM) and late-stage gametocytes (> 90 % stage IV/V, IC_{50} = 2464 nM) as before using luciferase expression as viability indicator[9] from *P. falciparum* NF54-*pfs16*-GFP-Luc[6] parasites.

ABS parasites, immature and late-stage gametocytes were treated with saponin (0.05 % (v/v), 10 min) followed by staining these parasites with TryphanBlue (0.2 % (w/v) at a 1:1 ratio to parasites) and visualized on a hemocytometer (40x magnification) as quantification of permeation into the different parasite stages.

Data analysis

Unless otherwise specified, all data are presented as the means from at least three independent experiments, each with technical triplicates, with the standard error of the mean (SEM) indicated. Statistical significance was determined with unpaired Student's *t*-test, one-way ANOVA and two-way ANOVA using GraphPad Prism (version 9) program.

References

1. Coetzee, N. *et al.* Epigenetic inhibitors target multiple stages of *Plasmodium falciparum* parasites. *Sci. Rep.* **10**, 1-11 (2020).

2. Ruecker, A. *et al.* A male and female gametocyte functional viability assay to identify biologically relevant malaria transmission-blocking drugs. *Antimicrob. Agents Chemother.* **58**, 7292-7302 (2014).

3. Cevenini, L. *et al.* Multicolor bioluminescence boosts malaria research: quantitative dual-color assay and single-cell imaging in *Plasmodium falciparum* parasites. *Anal. Chem.* **86**, 8814-8821 (2014).

4. Hasenkamp, S., Sidaway, A., Devine, O., Roye, R. & Horrocks, P. Evaluation of bioluminescence-based assays of anti-malarial drug activity. *Malar. J.* **12**, 1-10 (2013).

5. Zhang, J.-H., Chung, T. D. & Oldenburg, K. R. A simple statistical parameter for use in evaluation and validation of high throughput screening assays. *J. Biomol. Screen.* **4**, 67-73 (1999).

6. Adjalley, S. H. *et al.* Quantitative assessment of *Plasmodium falciparum* sexual development reveals potent transmission-blocking activity by methylene blue. *Proc Natl Acad Sci U S A* **108**, E1214-1223 (2011).

7. Verlinden, B. K. *et al.* Discovery of novel alkylated (bis) urea and (bis) thiourea polyamine analogues with potent antimalarial activities. *J. Med. Chem.* **54**, 6624-6633 (2011).

8. Reader, J. *et al.* Nowhere to hide: interrogating different metabolic parameters of *Plasmodium falciparum* gametocytes in a transmission-blocking drug discovery pipeline towards malaria elimination. *Malar. J.* **14**, 213 (2015).

9. Reader, J., Van Der Watt, M. & Birkholtz, L.-M. Streamlined and robust stage-specific profiling of gametocytocidal compounds against *Plasmodium falciparum*. *Front. Cell. Infect. Microbiol.* **12**, 859 (2022).

SUPPLEMENTARY FIGURES

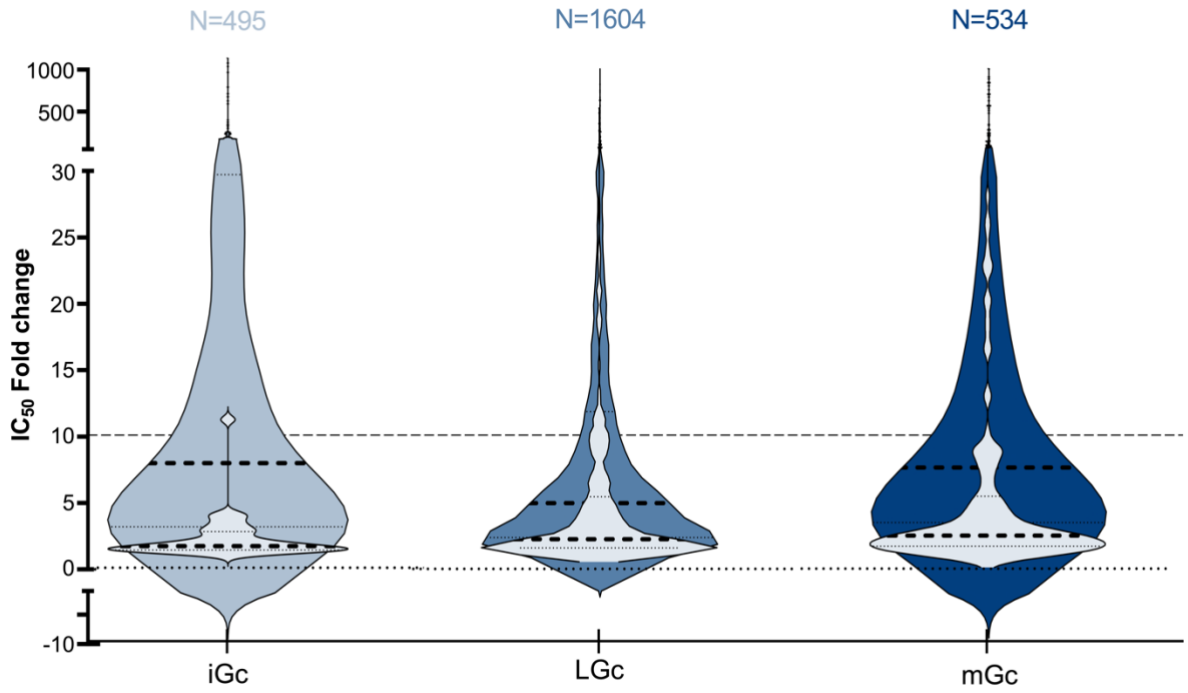

Supplementary Figure S1: Differences in activities indicated as fold change (FC) in IC_{50} between immature gametocytes (iGc) and asexual blood stage (ABS) parasites, late-stage gametocytes (LGc) and ABS parasites, and mature gametocytes (mGc) and ABS parasites. The lighter shaded area indicates preferential activity to gametocyte stages. Dark dashed lines indicate the median FC in each instance. Data are from published values, as shown in Supplementary File S1.

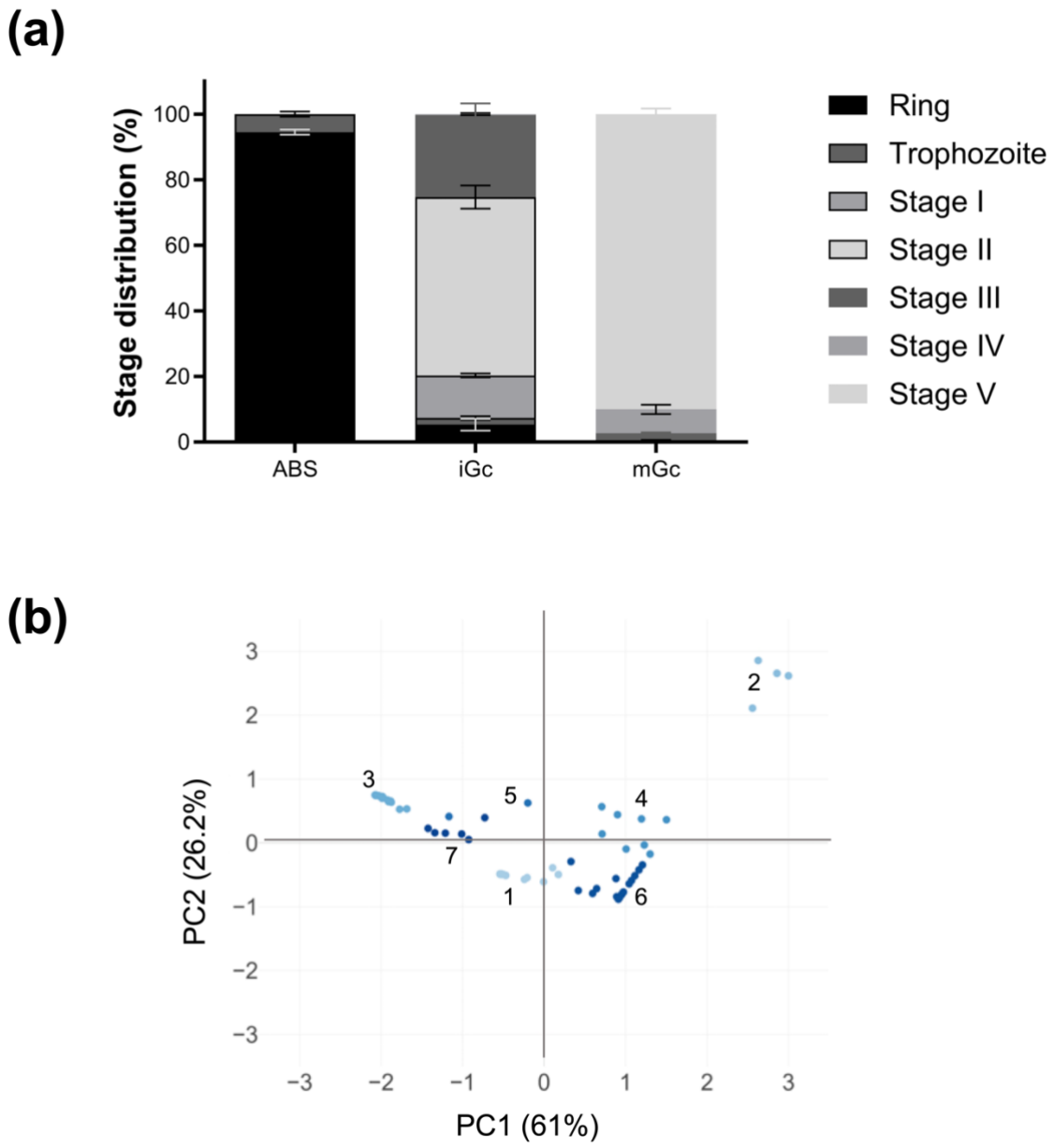

Supplementary Figure S2: Parallel evaluation of a select set of compounds against *P. falciparum*. a) Stage distribution of parasite populations used for screening compounds against asexual blood stage (ABS) parasites, immature gametocytes (iGc) and mature gametocytes (mGc). b) PCA of the K-means clustered activity profiles obtained.

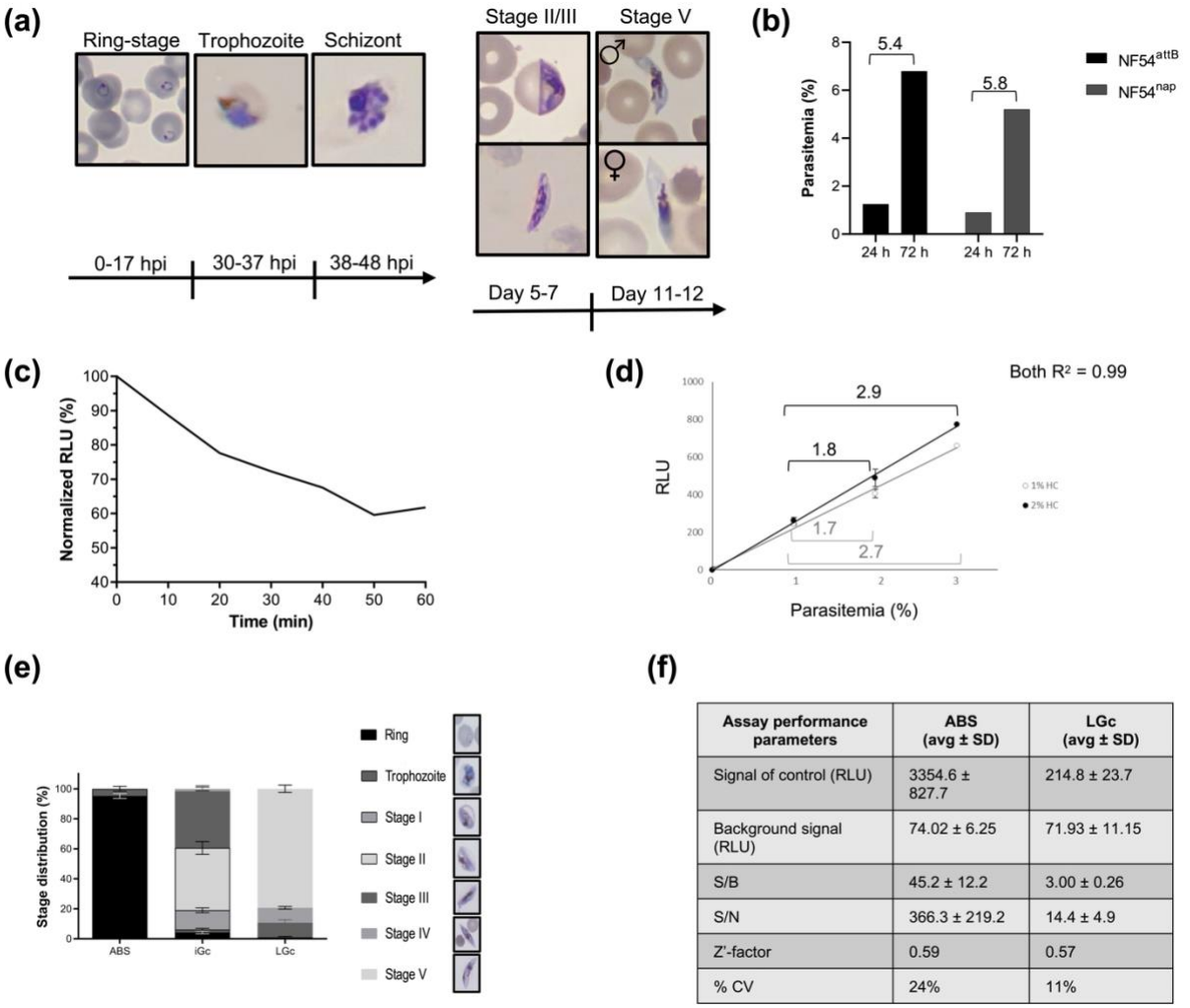

(f)

Assay performance parameters	ABS (avg ± SD)	LGc (avg ± SD)
Signal of control (RLU)	3354.6 ± 827.7	214.8 ± 23.7
Background signal (RLU)	74.02 ± 6.25	71.93 ± 11.15
S/B	45.2 ± 12.2	3.00 ± 0.26
S/N	366.3 ± 219.2	14.4 ± 4.9
Z'-factor	0.59	0.57
% CV	24%	11%

Supplementary Figure S3: a) Morphological evaluation of transgenic parasites in the ABS parasites and gametocyte development. ABS development of NF54^{nap} for the 48 h cycle were visualized by Giemsa-staining under a light microscope at 1000x magnification. Parasites develop into the ring stage between 0-17 hpi, to trophozoites (30-37 hpi) with an increase in the surface area of the cytoplasm. The final schizont stage (38-48 hpi) can be distinguished by a large, dense pigment vacuole and multiple nuclei being present that form merozoites (48 hpi). Gametocytogenesis of NF54^{nap} parasites were also visualized by Giemsa-staining under a light microscope at 1000x magnification. Committed ABS parasites undergo gametocytogenesis from day 1 to day 12 post-induction to develop into five distinct morphological stages. A D-shaped cytoplasm identifies stage II gametocytes and elongates further to form stage III gametocytes that were observed on days 5-7. Stage IV becomes sharp on both sides and distinguishes between male and female gametocytes. The gametocyte further matures into the transmissible stage V as notable by the round ends and a slight curve observed on day 10-12. b) Increase in parasitemia of NF54^{attB} (untransfected control) and NF54^{nap} ABS parasites. Synchronized parasites were monitored from ring-stage (0 h) and parasitemia was determined at 24 and 72 h (trophozoite stages). c) The normalized bioluminescent signal in relative light units (RLU) based on CBG99 activity was assessed at 10 min intervals over 1 h for the NF54^{nap} transgenic line at 6 % parasitemia (mixed population of rings and trophozoites) and 1 % hematocrit. d) Correlation of bioluminescent signal based on CBG99 luciferase activity for NF54^{nap} was measured at 1, 2 and 3 % parasitemia and 1 and 2 % hematocrit (HC) in 200 µL. The linear correlation (R^2) and fold change (FC) increases are shown (RLU, relative luminescence unit). e) The luciferase assay was performed after 96 h drug exposure for ABS parasites and 48 h for gametocytes. Stage distribution of parasite populations used for screening compounds against NF54^{nap} ABS parasites, iGc and LGc. F) The assay performance parameters were determined for data from 2-4 biological replicates performed in technical triplicates.

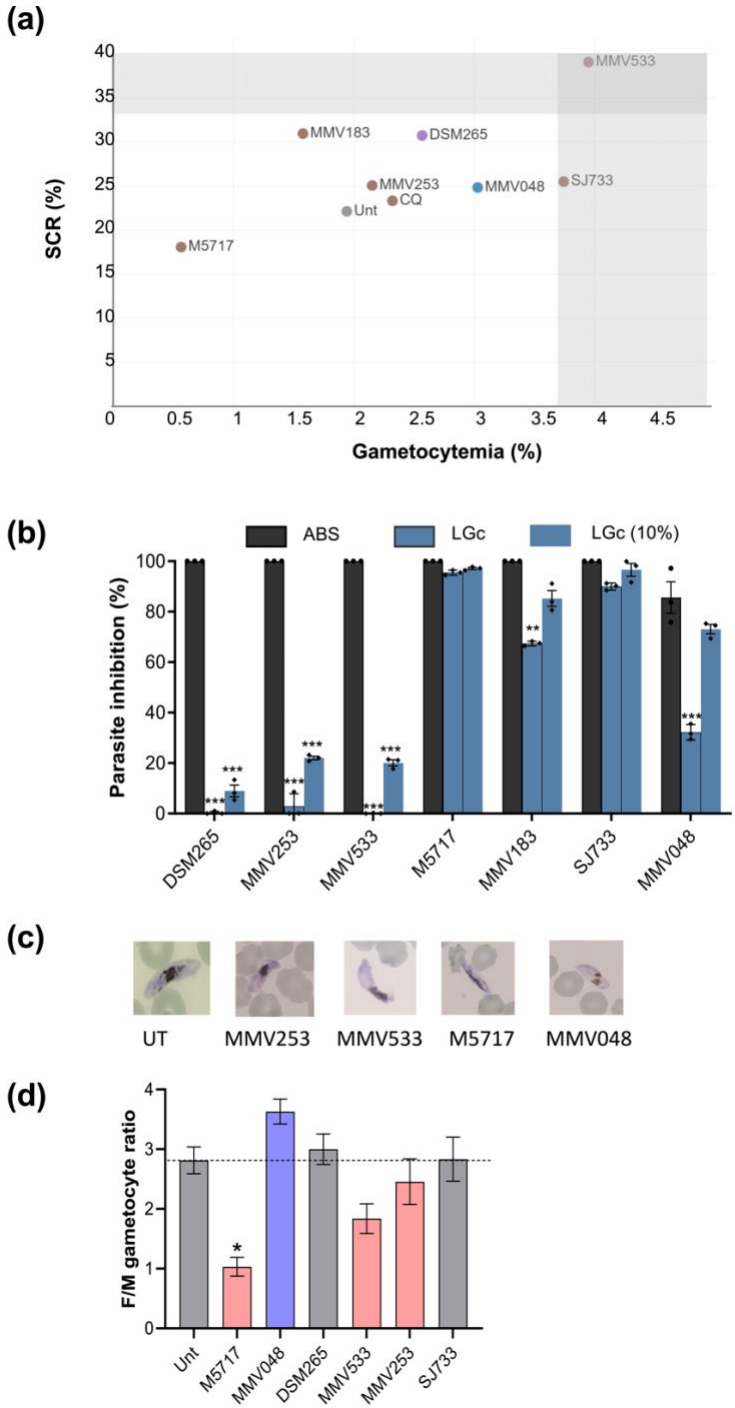

Supplementary Figure S4: a) Gametocyte commitment (calculated as the ratio of stage II gametocytes on day four to ring stage parasites on day two, expressed as percentage) relative to gametocyte production after treating ABS parasites at ABS IC_{50}. Gametocytemia (%) represents stage III gametocytes. Shaded areas indicate significant increases of parameters in comparison to untreated NF54 control. b) ABS parasites and late-stage gametocytes (LGc) populations at normal induced gametocyte numbers and adjusted to a 10 % of the normal gametocyte numbers treated at the therapeutic concentrations and inhibition measured with either SYBR Green fluorescence or luciferase expression after 48 h incubation. Data are from three independent biological repeats (n=3, mean ± SEM). Individual data points are indicated in symbols. Statistical evaluation was performed with one-way ANOVA (total DF = 8). c) Morphology of mature stage V gametocytes after a 48 h pulse on immature gametocytes. d) On day 13, the number of female to male gametocytes was determined using Giemsa-stained thin smear microscopy before investigating the viability of these gametocytes. Red bars indicate a reduction in number of female gametocytes counted and blue bars indicate a reduction in number of male gametocytes counted. Data are from two independent biological repeats (n=2, mean ± SEM). Statistical evaluation was performed with one-way ANOVA (total DF = 6).

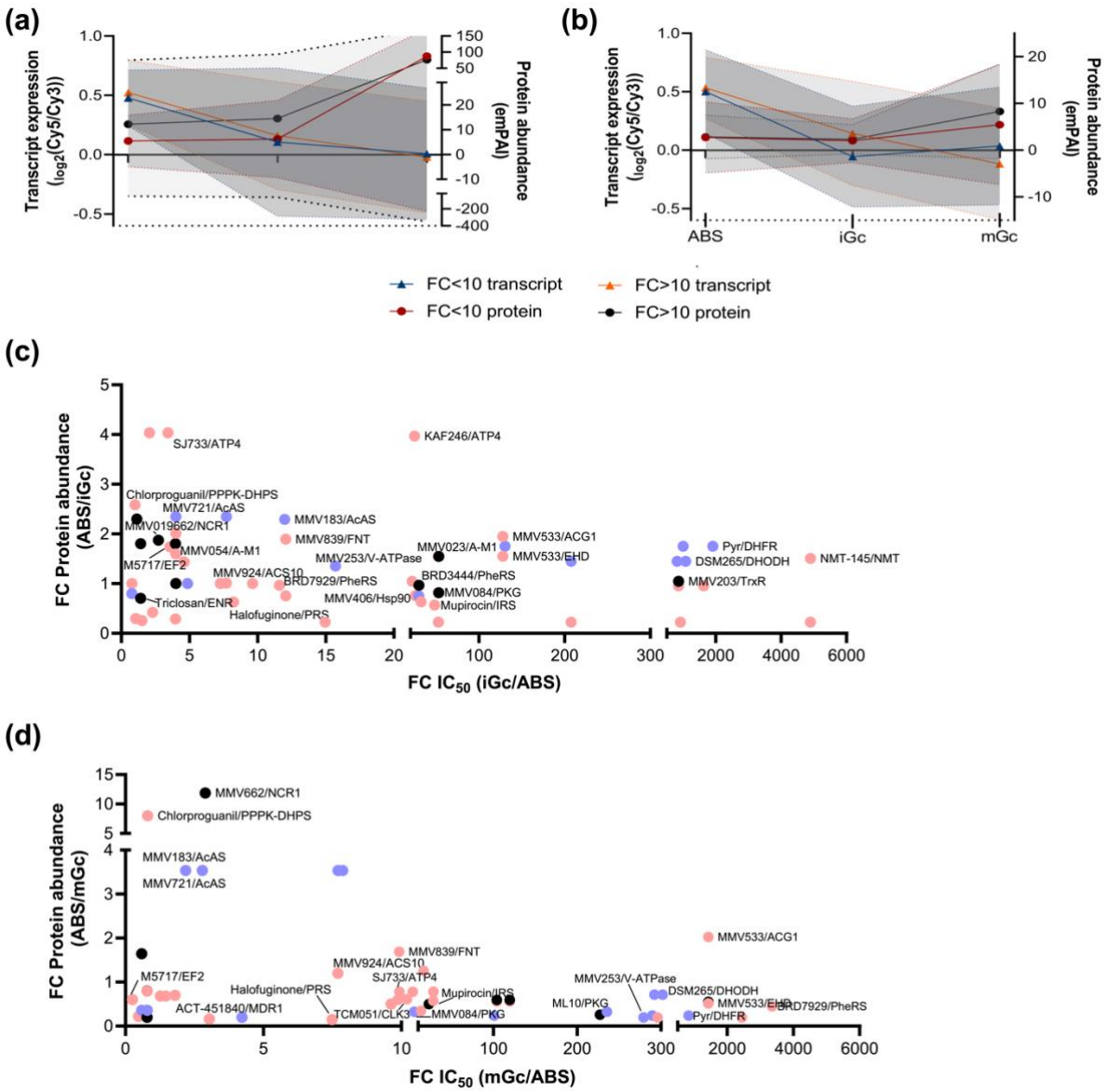

Supplementary Figure S5: Average transcript and protein expression of confirmed and/or implied targets of compounds with either maintained activity (FC < 10) or lost activity (FC > 10) from ABS parasites to either iGc (a) or mGc (b). Correlation between the FC in protein abundance and compound activity between (c) ABS parasites and iGc; and (d) ABS parasites and mGc. Blue indicates increased expression in male gametocytes, and pink shows increased expression in female gametocytes. AcAS, Acetyl-CoA synthetase; ACG1, aspartate-glutamate carrier isoform 1; ACS10, Acyl-CoA synthetase; A-M1, A-M1 alanyl aminopeptidase; CLK3, cyclin-dependent-like kinase; DHFR, Dihydrofolate reductase-thymidylate synthase; DHODH, Dihydroorotate dehydrogenase; EF2, Elongation factor 2; EHD, EH domain-containing protein; ENR, Enoyl-acyl carrier reductase; FNT, Formate-nitrite transporter; IRS, Isoleucine-tRNA synthetase; NCR1, Niemann-Pick type C1-related protein; NMT, N-myristoyltransferase; PheRS, Phenylalanine-tRNA synthetase; PKG, cGMP-dependent protein kinase; PPPK-DHPS, Hydroxymethyldihydropterin pyrophosphokinase-dihydropteroate synthase; PRS, Proline-tRNA synthetase; TrxR, Thioredoxin Reductase; V-ATPase, V-type ATPase.

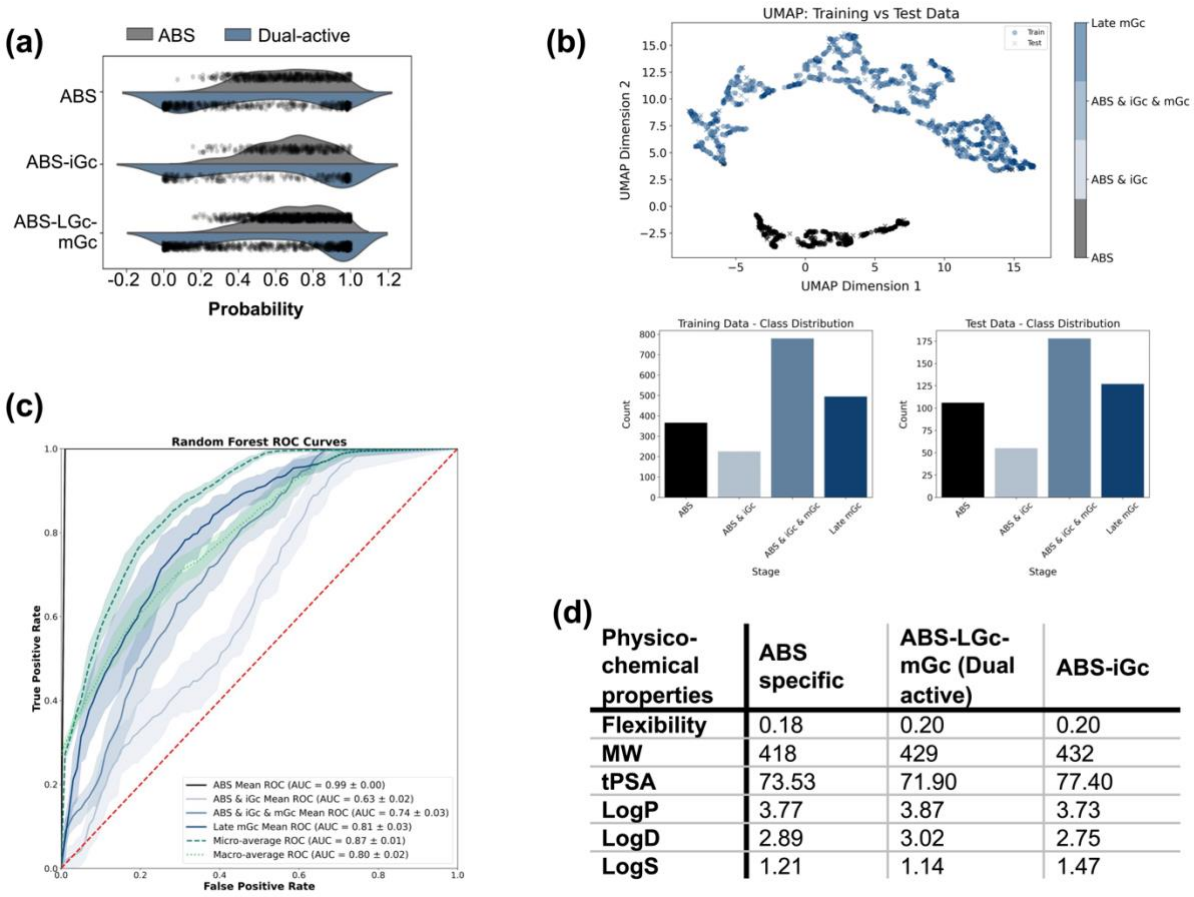

(d)

Physico-chemical properties	ABS specific	ABS-LGc-mGc (Dual active)	ABS-iGc
Flexibility	0.18	0.20	0.20
MW	418	429	432
tPSA	73.53	71.90	77.40
LogP	3.77	3.87	3.73
LogD	2.89	3.02	2.75
LogS	1.21	1.14	1.47

Supplementary Figure S6: Machine learning models to validate the stage-specific activity profiles of compounds. a) Probability scores were calculated in predicting combinations to show ABS parasite activity or dual activity against ABS parasites and gametocytes. b) Chemical space and class distribution of the training and test set data for model building and evaluation. c) ROC−AUC curves showing overall and class-wise performance of the random forest model in predicting compound stage-specificity when trained on the physicochemical properties of compounds after 10-fold cross-validation. Insert indicates AUC mean values ± standard deviation. d) Average values for the physicochemical properties for the different activity profile groups.

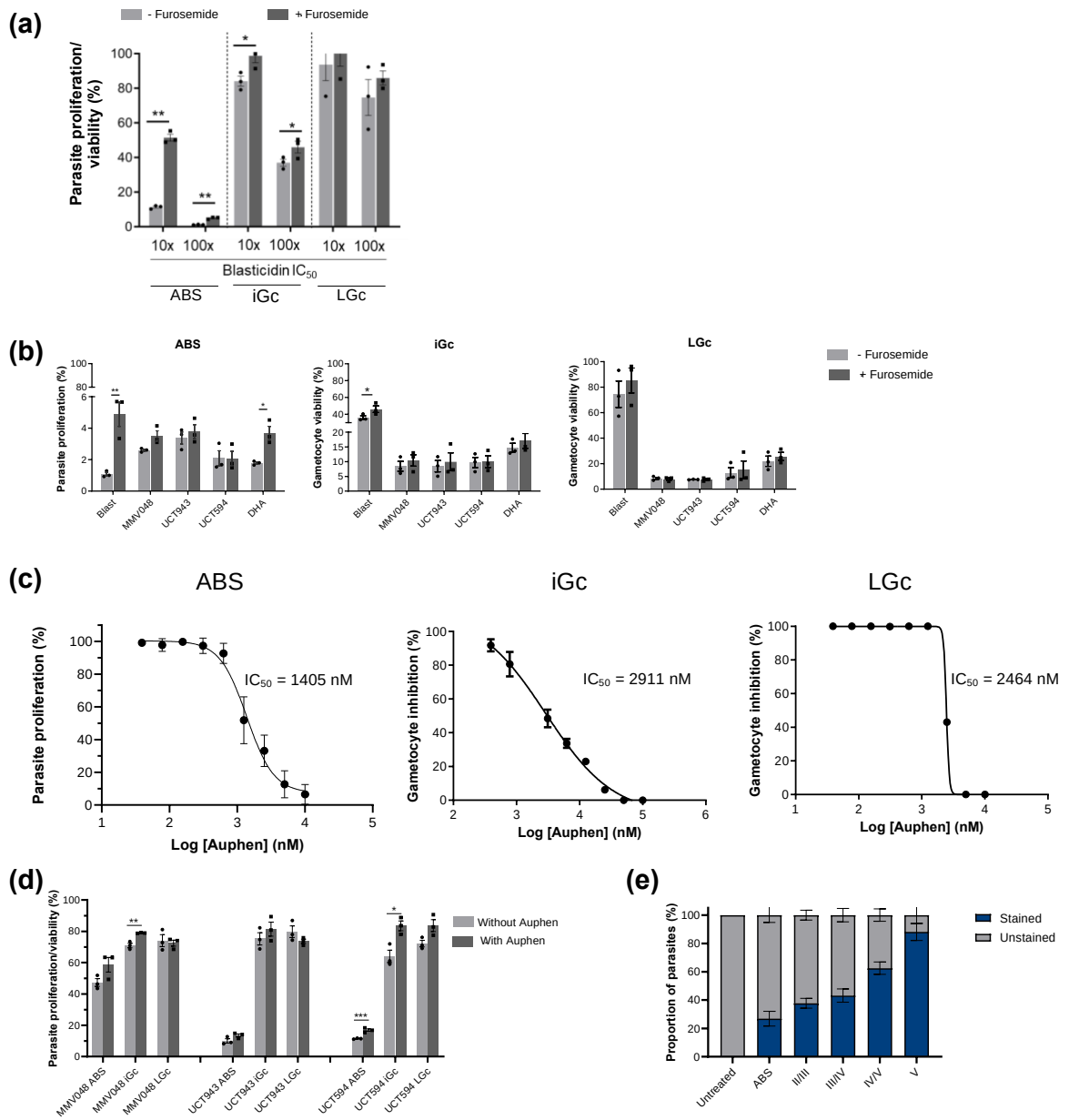

Supplementary Figure S7: a) The contribution of compound uptake through NPPs by confirming the set-up of this experiment by using Blasticidin (Blast) as positive control. ABS parasites, iGc and LGc (NF54^{nap} line) were either pre-treated with or without Furosemide (NPP blocker, 30 min) followed by treatment with Blast (at 10 x and 100 x IC_{50}) for a further 48 h and proliferation and viability measured with luciferase. Data are from three independent biological repeats (n=3, mean ± SEM). Statistical evaluation was performed with unpaired Student's *t*-test (df = 4). b) ABS parasites, iGc and LGc (NF54^{nap} line) were either pre-treated with or without Furosemide (NPP blocker, 30 min) followed by treatment with positive control (Blast), MMV048, UCT943, UCT594 and DHA for a further 48 h and proliferation and viability measured with luciferase. Data are from three independent biological repeats (n=3, mean ± SEM). Statistical evaluation was performed with unpaired Student's *t*-test (df = 4). c) Inhibition activity (IC_{50}) of only Auphen determined against ABS parasites (IC_{50} = 1405 nM), iGc (IC_{50} = 2911 nM) and LGc (IC_{50} = 2464 nM). d) ABS parasites, iGc and LGc (NF54^{nap} line) were either pre-treated with or without Auphen (AQP3 blocker, 30 min) followed by treatment with MMV048, UCT943 and UCT594 for a further 24 h and proliferation and viability measured with luciferase. Data are from three independent biological repeats (n=3, mean ± SEM). Statistical evaluation was performed with unpaired Student's *t*-test (df = 4). e) ABS parasites, iGc and LGc were treated with saponin (0.05 % (v/v), 10 min) followed by staining these parasites with TryphanBlue as quantification of permeation into the different parasite stages. Data are from two independent biological repeats (n=2, mean ± SEM).